Aromatic dialdehyde-based bisbenzoxazines: The influence of relative position of oxazine rings

Romain Tavernier[a], Lérys Granado[a], Gabriel Foyer[b], Ghislain David[a], Sylvain Caillol[a*]

[a] ICGM, Univ Montpellier, CNRS, ENSCM, Montpellier, France
[b] ArianeGroup, Rue de Touban, 33185 Le Haillan, France

Abstract

Polybenzoxazines are known to have superior thermal stability. Especially, the use of aromatic aldehydes instead of formaldehyde for the synthesis of benzoxazines monomers could improve this stability. However, the increase in aromatic content of the monomer can prevent the processability. The objective of this article is to understand the relationships between the conformation of an aromatic dialdehyde and its thermal properties. Two benzoxazine monomers were synthesized, based on salicylaldehyde, furfurylamine and respectively terephthalaldehyde (TPA, para configuration) and isophthalaldehyde (IPA, meta). Structural characterizations showed differences in intramolecular interactions between the two isomers. The melting transition of "meta" isomer was 50 °C lower than for "para" monomer, whereas polymerization temperatures and enthalpies were nearly the same. Volatile compounds released during the polymerization were the same in both cases, as investigated by mass spectrometry (Py-GC/MS). Curing kinetics using model-free kinetic methods revealed that the E-dependency follows the same trend for both monomers. Finally, thermal degradation monitored by thermogravimetric analysis under inert atmosphere was similar, with high degradation temperatures and high char yields (64%).

Keywords

Polybenzoxazines; Isoconversional analysis; High char yield; High performance thermoset

1. Introduction

Benzoxazines (BZX) are an interesting class of phenolic thermoset, which has gained increased attention during the last thirty years.[1] Their outstanding properties such as high thermal stability, initiator-free thermally activated polymerization and curing, and their relatively easy syntheses are some of the reasons that make BZX interesting from both academic and industrial communities. Among these properties of interest, the char formation at high temperature is desirable in the manufacturing of high performance thermosets, used in aerospace industry.[2] The particular structure of polymerizable benzoxazines is the arrangement of the oxazine ring relatively to the phenol, which confers the ability to polymerize. Only 1,3-benzoxazines undergo a specific ring-opening polymerization (ROP), due to the particular conformational structure of the heterocycle. Many studies have been conducted in order to understand the relationships between monomer design and subsequent properties of thermosets.[3–6]

For instance, Andreu *et al.* studied the effect of different substituents on the ring-opening polymerization of monobenzoxazines.[3] They showed that electronic effect of substituents on phenol and amine are of prime importance regarding the polymerization behavior. The polymerization temperature tends to decrease with stronger electron-withdrawing groups (EWG) in para position

relatively to phenol, whereas opposite trend is obtained with EWG groups in para position to the amine. In contrast, electron-donating groups showed only very slight effects. This study showed the importance of electronic environment regarding the mechanistic properties of benzoxazine polymerization.

More recently, Kolanadiyil *et al.* investigated the role of the number of oxazine moieties per monomer in the ring-opening polymerization behavior.[7] Hence, higher functionality was shown to lower polymerization temperatures and to enhance the thermal stability. It also reduced the volatilization of benzoxazine fragments during the polymerization. However, the increase of the number of oxazine rings also required longer curing times (or higher temperature). Thus, it has been suggested that the functionality dictates the curing behavior and final properties. Usually, bisbenzoxazines – comprising two oxazine rings per monomer, are used to ensure complete crosslinking of polymers, since monobenzoxazines are known to yield only low molar mass polymers. This effect has been attributed to a terminating effect of hydrogen bonding.[8]

In another research article, Kolanadiyil *et al.* studied the influence of relative position of the two oxazine rings on polymerization of bisbenzoxazines.[9] They synthesized three bisbenzoxazines with different oxazine-ring relative positions, *i.e.* one bisbenzoxazine having another oxazine ring attached in ortho position to the phenol moiety of the first benzoxazine, and two others with para and meta-substitution. They showed that ROP temperature was influenced by these relative positions. Firstly, intermolecular interactions were related to configuration, influencing hydrogen bonds. Secondly, intramolecular interactions were also affected, with the electronic effects of the attached rings impacting the opening of the other rings. The meta position seemed to be the most affected by the relative position of the rings, because it was supposed to have a catalytic effect both by the intramolecular proximity of the polymerizable moieties and by intermolecular assistance of hydrogen bonding which has been shown for some other benzoxazines. This strong reactivity of meta structural configuration has also been confirmed with resorcinol-based and meta-phenylenediamine-based benzoxazines.[10–12]

Bisbenzoxazines based on isomers of bisphenol F have been studied by Liu and Ishida, and an unexpected effect on glass transition temperatures, T_g, has been observed.[13] The three isomers of this bisphenol, *i.e.* ortho-ortho, para-para and ortho-para led to differences in T_g that appeared unusual. Indeed, usually, “para” configured polymers display higher T_g than “ortho” configured chains. In their work, ortho-ortho configuration of bisphenol F led to polybenzoxazines with higher T_g, higher crosslinking density and higher degradation temperature. These findings underlined the absolute necessity of controlling the molecular design to tune the final thermoset properties.

Recently, the trend toward the use of safer chemicals led to the development of new chemistries for thermosets. For example, cyclic carbonates are replacing isocyanates for polyurethanes,[14] biobased compounds are looked forward to replace bisphenol A and aromatic amines in polyepoxides,[15,16] and new phenols and aldehydes have shown promising properties as an alternative to formophenolics.[17] In this context, the use of aromatic aldehydes in substitution of formaldehyde provides new possibilities for the synthesis of polybenzoxazines. Ohashi *et al.* reported the first formaldehyde-free synthesis of 2-subtituted benzoxazine monomers[18] and in a previous article, we provided deeper insights into ROP mechanisms of these new benzoxazines.[19] Our study suggested that 2-substituted benzoxazines exhibit similar polymerization behavior and analogous network

structures than 1,3-*2H*-benzoxazines. The reactivity of these benzoxazines with higher substitution on the oxazine ring provided a new way to obtain bifunctional monomers, by the use of dialdehydes instead of diphenols or diamines.

In the present article, we aim to study the effect of relative position of the oxazine ring by the use of different phthalic aldehydes that are drastically less toxic than formaldehyde, *i.e.* terephthalaldehyde (TPA) with two aldehydes in *para* position and isophthalaldehyde (IPA) which has a *meta* configuration. We synthesized two bisbenzoxazines using the same synthetic pathway and studied their polymerization behavior, through a thermo-kinetic study carried out using infrared spectroscopy, differential scanning calorimetry and isoconversional computations. The final thermal performances of the two BZX were compared. Overall, we provide herein some new insights into the structure-properties relationships of these difunctional benzoxazines.

2. Experimental

2.1. Materials

Salicylaldehyde, terephthalaldehyde, isophthalaldehyde and furfurylamine were purchased from TCI. Sodium borohydride was purchased from Sigma-Aldrich. Anhydrous magnesium sulphate, acetone, methanol, ethyl acetate and absolute ethanol were purchased from VWR. Deuterated chloroform was purchased from Eurisotop. All solvents and reagents were used without further purification.

2.2. Synthesis of Furfurylaminomethylphenol (Scheme 1, FA)

In a round-bottom flask, salicylaldehyde (20.0 g, 164 mmol) was dissolved in 100 mL of methanol and then furfurylamine (15.9 g, 164 mmol) was added to the solution. The mixture was heated in a thermostated oil bath to reflux for 1.5 h. After cooling to room temperature, solvent was removed under reduced pressure in order to isolate furfuryliminomethylphenol (FI) and for characterization purpose. Then, FI was dissolved in 75 mL of methanol and 6.20 g (164 mmol) of $NaBH_4$ were added in small portions, starting at 0 °C. After complete addition of $NaBH_4$, the mixture has been heated to reflux for 2 h. In order to quench $NaBH_4$ residues, the mixture has been precipitated against 600 mL of distilled water. A viscous oil was formed in suspension in water, and it was extracted twice with 250 mL of ethyl acetate, washed with distilled water, and the organic phase was dried on magnesium sulfate and concentrated under vacuum. The resulting brown oil was then dried under vacuum at 40°C overnight. 29.6 g of the desired product has been recovered (88% yield).

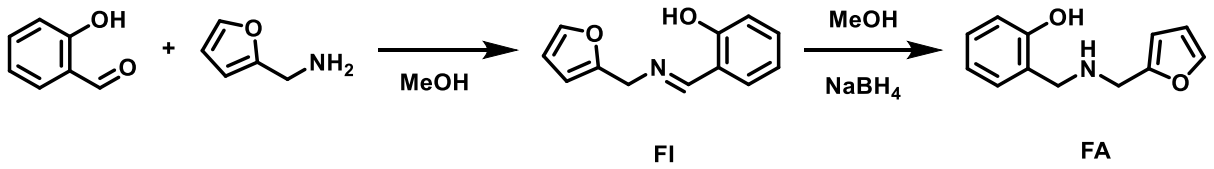

Scheme 1 - Reaction scheme for the synthesis of Furfurylaminomethylphenol

FI (imine): ^{1}H NMR ($CDCl_3$, 7.26 ppm) δ 8.38 (t, 1H, ^{3}J=1.1 Hz), 7.40 (dd, 1H, ^{3}J=1.85 Hz, ^{4}J=0.9 Hz), 7.35-7.30 (ddd, 1H, ^{3}J=9.3 Hz, ^{4}J=7.3 Hz, ^{5}J=9.3 Hz), 7.25 (1H, dd, ^{3}J=7.7 Hz, ^{4}J=1.9 Hz), 6.99-6.97 (ddd, 1H, ^{3}J=8.4 Hz, ^{4}J=0.9 Hz, ^{5}J=0.4 Hz), 6.91-6.87 (m, 1H), 6.36 (dd, 1H, ^{3}J=3.4 Hz, ^{4}J=1.9 Hz), 6.28 (m, 1H), 4.76 (s, 2H).

FA (amine) : ^{1}H NMR ($CDCl_3$, 7.26 ppm) δ 7.40 (dd, 1H, ^{3}J=1.9 Hz, ^{4}J=0.9 Hz), 7.21 (m, 1H), 6.99-6.96 (m, 1H), 6.86 (dd, ^{3}J=8 Hz, ^{4}J=1.1 Hz), 6.81-6.77 (td, 1H, ^{3}J=7.5Hz, ^{4}J=1,3 Hz), 6.34 (dd, 1H, ^{3}J=3.2 Hz, ^{4}J=1.9 Hz), 6.21 (m, 1H), 3.96 (s, 2H), 3.82 (s, 2H).

HRMS (*m/z*, positive mode, $[M + H]^+$): $C_{12}H_{14}NO_2$; calculated 204.1019, found 204.1027.

2.3. Synthesis of benzoxazine monomers

Ph-fa[2,2']tpa: 4.00 g (19.7 mmol, 2 eq) of furfurylaminomethylphenol (FA) and 1.31 g (9.80 mmol, 1 eq) of terephthalaldehyde were dissolved in 3 mL of acetone in a glass vial. The mixture has been stirred with a magnetic stirrer for 1 h. After few minutes, a white solid precipitated, but the mixture has been kept stirring at ambient temperature in order to ensure maximum precipitation of the product. The solid was recovered by filtration and washed with acetone, affording 4.02 g of the desired product (after overnight vacuum drying at 40°C). Yield = 82%.

^{1}H NMR ($CDCl_3$, 7.26 ppm) δ 7.64 (d, 4H), 7.40 (s, 2H), 7.18 (td, 2H), 6.98 (dt, 2H), 6.93 (d, 2H), 6.88 (tt, 2H), 6.32 (q, 2H), 6.21 (m, 2H), 5.98 (2 s, 2H), 3.95 (m, 4H), 3.82 (s, 4H).

^{13}C NMR ($CDCl_3$, 77.16 ppm) δ 153.56, 153.53, 152.31, 142.45, 142.44, 138.61, 138.58, 128.00, 127.78, 126.90, 120.88, 119.55, 119.54, 116.66, 110.26, 108.67, 108.65, 90.01, 89.95, 47.36, 47.35, 46.41, 46.35.

HRMS (*m/z*, positive mode, $[M + H]^+$): $C_{32}H_{29}N_2O_4$; calculated 505.2127, found 505.2126.

Ph-fa[2,2']ipa: 4.00 g (19.7 mmol, 2 eq) of furfurylaminomethylphenol (**FA**) and 1.30 g (9.70 mmol, 1 eq) of isophthalaldehyde were dissolved in 3 mL of ethanol in a glass vial. The mixture has been stirred with a magnetic stirrer for 1h. After few minutes, a brown precipitate appears which then redissolved. Another precipitation occurred during the stirring and the solid did not redissolved. After 1 h hour stirring, the solid was recovered by filtration and washed with ethanol. The recovered solid was then recrystallized in ethanol, and the resulting compound was then dried under vacuum overnight at 40 °C. 3.39 g of product was afforded as a white solid. Yield = 69 %.

^{1}H NMR ($CDCl_3$, 7.26 ppm) δ 7.91 (s, 1H), 7.59 (d, 2H), 7.40 (d, 1H), 7.38 (dd, 1H), 7.36 (dd, 1H), 7.17-7.22 (m, 2H), 6.97-7.00 (dd, 2H), 6.87-6.95 (m, 4H), 6.30-6.32 (m, 2H), 6.22 (dd, 1H), 6.18 (dd, 1H), 6.00 (s, 1H), 5.98 (s, 1H), 6.79-4.01 (m, 4H), 3.80 (s, 4H).

^{13}C NMR ($CDCl_3$, 77.16 ppm) δ 153.65, 153.60, 152.45, 152.41, 142.34, 138.94, 138.89, 128.65, 128.63, 127.96, 127.76, 126.65, 125.40, 125.38, 120.87, 120.84, 119.61, 119.60, 116.74, 116.72, 110.28, 110.26, 108.56, 108.53, 90.19, 90.17, 47.56, 47.51, 46.29, 46.12.

HRMS (*m/z*, positive mode, $[M + H]^+$): $C_{32}H_{29}N_2O_4$; calculated 505.2127, found 505.2123.

2.4. Measurements

NMR spectroscopy has been performed using a Bruker AC 400 NMR spectrometer. Chemical shift reference was determined using residual non deuterated solvent.

Fourier transform infrared absorption spectroscopy (FTIR) measurements were performed on a Nicolet 6700 spectrometer (Thermo-Scientific), with a mercury−cadmium−tellurium detector, resolution was 4 cm^{-1} and 32 scans were added for each spectrum.

High Resolution Mass Spectrometry measurements (HRMS) for synthesized compounds were done on a Waters Synapt G2-S High Resolution Mass Spectrometer. An electrospray ionization (ESI) method was used.

Differential scanning calorimetry (DSC) were performed on a DSC-3 F200 Maia from Netzsch GmbH. The machine is equipped with an intracooler module. Nitrogen flow used was 70 mL·min^{-1}. The temperature sensor was calibrated with biphenyl, indium, bismuth, and CsCl high purity standards at 10 °C·min^{-1}. In order to prevent volatile evaporation, high-pressure stainless- steel pans and lids sealed at 3 N·cm were used.

Dry content was measured after curing at 200°C. Between 90 and 125 mg of sample were cured in aluminum pans and weighed after curing. The dry content is the weight loss that happened during curing. It is presented as an average of 4 samples for each monomer.

Thermogravimetric analyses (TGA) were performed with a TGA-3 Libra (Netzsch).Alumina crucibles were used. Samples used were weighed between 10 and 12 mg, and introduced as monoliths.The heating rates were 10 °C·min^{-1} from RT to 900 °C. All TGA analyses were performed under 40 mL·min^{-1} nitrogen flow.

Py-GC/MS setup: Compounds were pyrolyzed with a Pyroprobe 5000 pyrolyzer (CDS Analytical) under a helium flow. The pyrolyzer sample holder consists in a quartz tube equipped with an electrically heating platinum filament. Less than 1 mg of sample is placed into the quartz tube, between two pieces of quartz wool. Pyrolyzis was enabled by a coil probe. Successive pyrolysis step were done at 200, 300, 400, 500, 600 and 900 °C. Each temperature was held for 15 s before gases were drawn to the GC for 5 min. The pyrolyzer was coupled to a 450-GC gas chromatograph (Varian) by means of a transfer line heated at 270 °C. The GC oven initial temperature of 70 °C was held for 0.2 min, and then raised to 310°C at 10 °C·min^{-1}. GC column was a Varian Vf-5 ms capillary column (30 m × 0.25 mm) and the carrier gas was helium (1 mL·min^{-1}); a split ratio was set to 1:50. The MS analyzer used was an ion trap analyzer (240-MS from Varian) directly coupled to the capillary column. Identification of the products was achieved using the American National Institute of Standards and Technology mass spectral library.

2.5. Thermo-kinetics analysis

The isoconversional computations were performed from non-isothermal DSC data, at different heating rates: β = 5.0, 7.5, 10.0, 12.5 and 15.0 °C·min^{-1}. The degree of curing, α, was calculated from the time-integration of exothermic peak with respect to the overall curing enthalpy ($\alpha = \Delta H_t/\Delta H_{TOTAL}$). A simple straight-line approximation was taken to draw the baseline for integration. The activation energy values were calculated as a function of α, using custom-made programs. Differential Friedman and integral Vyazovkin approaches were used. The theoretical considerations and computational detail can be found in our previous articles.[17,20,21]

3. Results and discussion

3.1. Monomer syntheses and characterizations

Bisbenzoxazines based on aromatic dialdehydes have been synthesized in three steps, according to our previous work. Furfurylamine was reacted with salicylaldehyde, in order to obtain an imine, which was then reduced by sodium borohydride. The obtained secondary amine, furfurylaminomethylphenol (**FA**) was then reacted with corresponding aldehyde, as shown in Scheme 2. Respectively 1 equivalent

of terephthalaldehyde (TPA, para) or isophthalaldehyde (IPA, meta) was reacted with 2 equivalents of furfurylaminomethylphenol, to get corresponding bisbenzoxazines. According to the abbreviations introduced by Ohashi *et al.* and our previous contribution, para oriented benzoxazine is **Ph-fa[2,2']tpa** and meta is **Ph-fa[2,2']ipa**.[18]

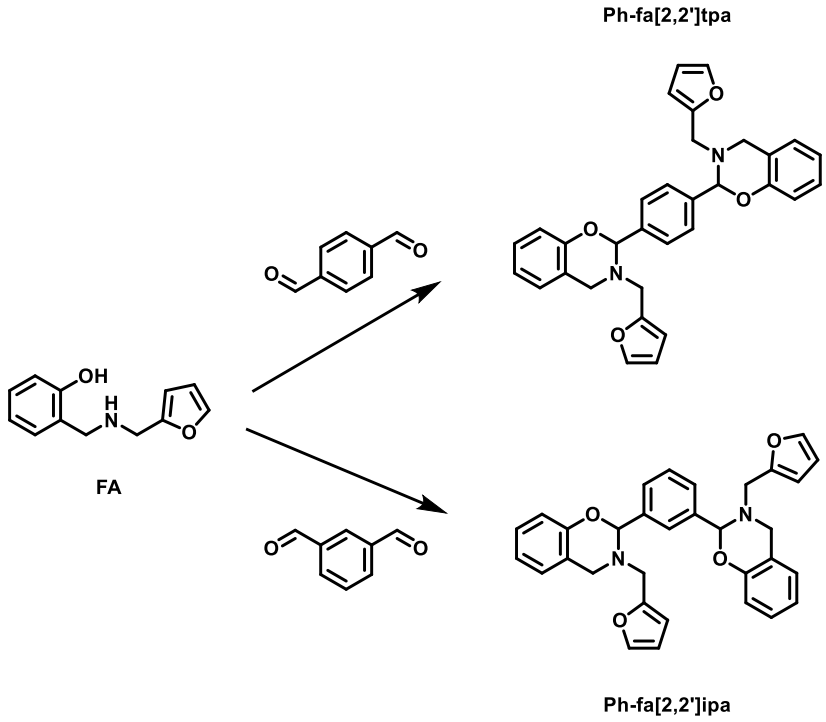

Scheme 2 - Reaction scheme for the synthesis of dialdehyde-based benzoxazines

Reaction occurred for all monomers at ambient temperature, within a few minutes. Product recovery was easier by choosing the appropriate solvent. Indeed, we performed the syntheses in a non-solvent of the final product. Before optimization, reactions had been performed first in refluxing toluene, and precipitation was observed for **Ph-fa[2,2']tpa** but not for **Ph-fa[2,2']ipa** (results not shown). Reaction conditions have then been adapted in order to get the corresponding monomers in milder and more convenient conditions. Monomer solubilities were different, **Ph-fa[2,2']tpa** being insoluble in acetone, whereas **Ph-fa[2,2']ipa** was soluble in acetone, toluene and insoluble in ethanol. We thus selected respectively acetone and ethanol as reaction medium, since desired products are insoluble in these solvents. Hence, they precipitated when formed and could be recovered by simple filtration.

Structural characterizations of the monomers have been performed by ^{1}H and ^{13}C NMR spectroscopies. ^{1}H NMR spectroscopy, displayed in Figure 1-a, revealed the presence of diastereomers. Indeed, the signal OCH(Ar)N (a and a') is observed as two singlets for both monomers, at 5.98 ppm for **Ph-fa[2,2']tpa** and 6.00 ppm for **Ph-fa[2,2']ipa**. Aromatic protons from aryl attached to the two oxazine rings in **Ph-fa[2,2']tpa** is also observed as two singlets, at 7.64 ppm whereas in **Ph-fa[2,2']ipa**, these protons are not equivalent. The signal from aromatic proton located between the two bonds attaching the oxazine rings (i) is observed as a singlet at 7.94 ppm and other protons from the aromatic ring (g and h) are observed respectively at 7.41 (1H, d) and 7.59 (2H, d). Protons from furan rings are also influenced by the conformation of the monomer. When oxazine rings are attached in *para* position, furan ring protons are equivalent in both diastereomers (d', e' and f'), and they are observed

respectively at 6.21, 6.32 and 7.40 ppm. However, when the rings are bonded in meta position, some furan rings protons have different chemical shifts. We can explain this observation by the fact that dangling furan rings may interact with aryl protons, but only in **Ph-fa[2,2']ipa**. Indeed, the closest furan proton to the IPA residue (proton d) is observed at 6.18 and 6.22 ppm. Its neighboring proton (e) is observed at 6.30 ppm as a unique (but complex) signal. The furthest furan proton is also affected and observed as two signals, at 7.37 and 7.38 ppm. The free rotation of the furan ring due to the methylene bond, can explain these strong interactions on protons d and f, and weaker one on proton e.

Infrared spectroscopy has also been performed on monomers and results are shown in Figure 1-b. According to the literature, Ar-O phenolic bands are observed at 1217 and 1035 cm^{-1} for **Ph-fa[2,2']tpa** and at 1230 and 1035 cm^{-1} for **Ph-fa[2,2']ipa**. Moreover, the specific benzoxazine band is observed as a broad band in **Ph-fa[2,2']tpa** at 938 cm^{-1}, corresponding to the O-C-N bonds. This broad band may be explained by the existence of diastereomers, as we reported before and according to the NMR spectroscopy results. **For Ph-fa[2,2']ipa**, several bands are observed in the region of the O-C-N bond vibration. Three main bands are observed at 951, 926 and 909 cm^{-1}. This more complex behavior is in line with the NMR spectroscopy results, confirming that the presence of diastereomer has more influence in **Ph-fa[2,2']ipa** than in **Ph-fa[2,2']tpa** due to the non-symmetrical character of the molecule. Finally, the sharp peaks at 1584 cm^{-1} for **Ph-fa[2,2']tpa** and 1582 cm^{-1} for **Ph-fa[2,2']ipa** are characteristic of the furan ring.[22–25]

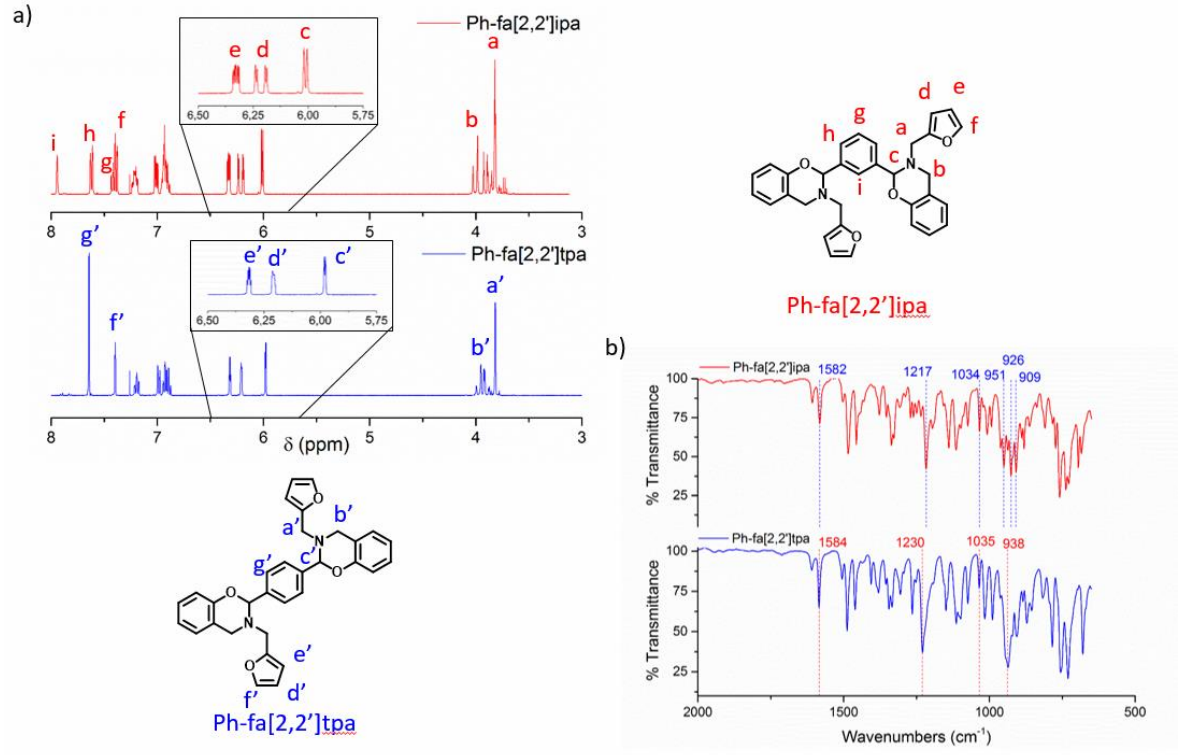

Figure 1 - a) NMR 1H spectra and ; b) FT-IR spetra of both monomers Ph-fa[2,2']ipa and Ph-fa[2,2']tpa

3.2. Curing kinetics

Figure 2 depicts the DSC thermograms of **Ph-fa[2,2']tpa** and **Ph-fa[2,2']ipa**, recorded at 10 °C·min^{-1}. A sharp endothermic peak is observed at 164 °C for **Ph-fa[2,2']tpa**, corresponding to the melting transition of monomers. **Ph-fa[2,2']ipa** behaved differently, with a melting temperature at 112 °C, which can be explained by the effect of the isomerism. Even after recrystallization, the melting endotherm of **Ph-fa[2,2']ipa** is broad, indicating that the crystalline network is less ordered than in **Ph-fa[2,2']tpa**. The arrangement of different rings in the monomer could partially prevent the crystallization, thus requiring less energy to melt the compound. Polymerization occurred for both monomers, resulting in exothermic peaks in the thermograms, with an onset at 216 °C and maximum at 235 °C for **Ph-fa[2,2']tpa** and an onset at 212 °C and maximum at 249 °C for **Ph-fa[2,2']ipa**. These very similar values were expected, since the configuration of both oxazine rings are the same within each monomer structure. Indeed, oxygen and nitrogen atom of each ring are attached to the same aromatic ring, symmetrically. The work of Kolanadiyil *et al.* was based on isomeric benzoxazines which displayed very different electronic configuration for each ring in all their 3 monomers, and they consequently observed different polymerization temperatures.[9] Polymerization enthalpies are also found rather similar, namely 257 and 278 J·g^{-1} for **Ph-fa[2,2']tpa** and **Ph-fa[2,2']ipa,** respectively. However, a slight difference is observed in the shape of the polymerization peaks. **Ph-fa[2,2']tpa** displays a large peak, with a small shoulder after the peak maximum, whereas **Ph-fa[2,2']ipa** displays a clear bimodular peak. In addition for **Ph-fa[2,2']ipa**, the maximum heat flux (peak maximum at which the reaction rate is the fastest) occurs during the second phenomenon, with a difference of 14 °C observed between the two monomers peak maxima. This bimodular behavior can find an explanation in the fact that each monomer is a mixture of two diastereomers, which may display slightly different polymerization behaviors. It is unlikely that each of the two rings will ring-open owing to different ways. Indeed, in that case, such this behavior should have been observed by Kolanadiyil *et al*. with monomers with higher functionalities.[7] In our last article, we reported polymerization behaviors of several 2-substituted benzoxazines.[19] One of them displayed two partially separated polymerization enthalpies, for a symmetric monomer, that was also a mixture of diastereomers. Thus, the influence of the presence of diastereomers is likely to explain our observations. However, the study of diastereomerically pure samples would bring more insights into this phenomenon. Overall, DSC study of the monomers led to the conclusion that both monomers had nearly the same polymerization behavior. However, the advantage of **Ph-fa[2,2']ipa** is the larger processing window, with a favorable difference of nearly 100 °C between melting point and polymerization onset, compared to **Ph-fa[2,2']tpa** that has a theoretical processing window of only 50 °C.

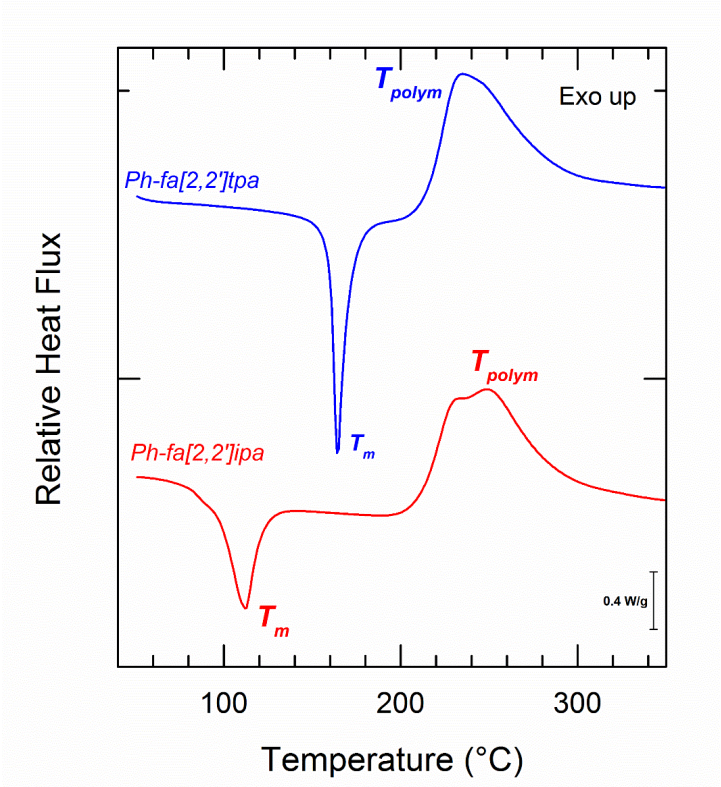

Figure 2 -- DSC of Ph-fa[2,2']ipa and Ph-fa[2,2']tpa at 10 °C·min^{-1}

In order to get more insights about the crosslinking mechanisms, a kinetic analysis was performed, using a model-free kinetic method. We used non-isothermal differential scanning calorimetry integral and differential data, with multiple heating rates. The advanced isoconversional method of Vyazovkin[26] has been used and compared with results obtained with Friedman's method.[27] This kinetic analysis is based on the elucidation of activation energy, as described by Arrhenius equations. Isoconversional kinetic analysis has proven to be very useful in the elucidation of curing mechanisms.[28] Figure 3-a depicts the degree of curing as a function of temperature, at different heating rates for both **Ph-fa[2,2']tpa** and **Ph-fa[2,2']ipa**. We can observe that for all heating rates, kinetic profiles are parallel. This confirms that generated data can be used for isoconversional analysis.

Reaction rate as a function of crosslinking degree is shown in Figure 3-b for both monomers, at different heating rates. We can observe two shifts of the reaction rates, occurring for **Ph-fa[2,2']tpa** and **Ph-fa[2,2']ipa** at the same conversion, for all heating rates. Three regimes can thus be ascribed for these polymerizations. The first regime occurred for $\alpha < 0.25$, which is thought to correspond to the initiation of the ROP and starting of the propagation of reactive species in the network. For $0.25 < \alpha < 0.55$, we observe a transient regime, with a slower rate, corresponding to the propagation of polymerization. For $\alpha > 0.55$, reaction rate drastically reduces, and this corresponds to a limitation of the diffusion of reactive species, due to an increase of the viscosity. These different regimes happen at the same conversion for both monomer. However, at low conversion, the increase of reaction rate

is more important for **Ph-fa[2,2']tpa**, than for **Ph-fa[2,2']ipa**. This can be explained by the less hindered *para* structure, which facilitates the efficient collisions of molecule, and thus the diffusion.

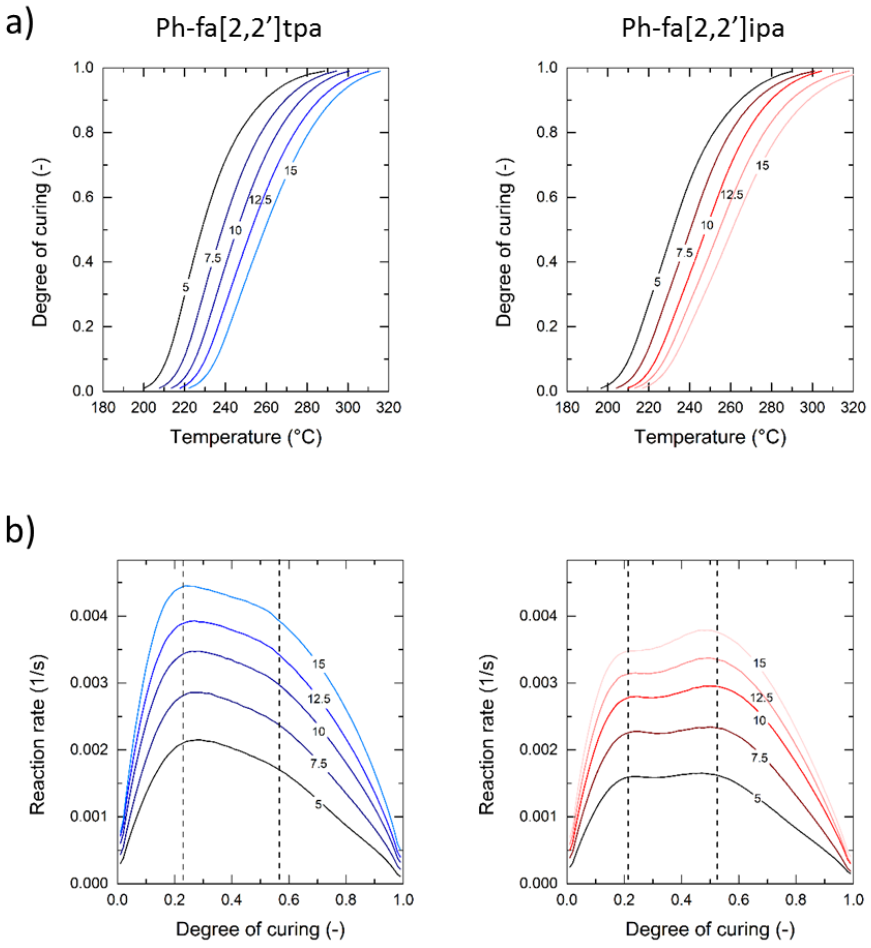

Figure 3 - a) Degree of curing as a function of temperature and - b) Reaction rate as a function of degree of curing for Ph-fa[2,2']ipa and Ph-fa[2,2']tpa

Activation energy, E_a, as a function of crosslinking degree is shown in Figure 4. For both monomers, activation energy ranges between 55 and 103 kJ·mol^{-1}. At low conversion ($\alpha < 0.25$), E_a decreases to reach a plateau for $0.25 < \alpha < 0.55$, and then it increases toward the end of reaction. At low conversion, a decrease in the activation energy is observed with increasing conversion. This could be explained by the fact that the ring-opening is a high energy barrier to overcome. As the conversion from unreacted to ring-opened monomer increases, the energy barrier decreases, represented by the decrease in activation energy. The plateau for $0.25 < \alpha < 0.55$ with the lowest activation energy for both monomers, *i.e.* 55 kJ·mol^{-1} for **Ph-fa[2,2']tpa** and 65 kJ·mol^{-1} for **Ph-fa[2,2']ipa** could represent a transient regime. During this regime, polymerization seems limited neither by diffusion of reactive species nor gelation. It can be mentioned that for $\alpha < 0,8$, the calculated E_a for the *para* monomer is lower than for the *meta* monomer, and it could be due to a lower steric hindrance for the *para* position. At the end of the curing reaction, E_a increases, as generally observed because the reaction is diffusion-controlled. This is also illustrated by the lower confidence in calculated values (Figure S13), especially for **Ph-fa[2,2']ipa** that shows an important lowering of the correlation coefficient. This is however the only significant difference of reactivity observed between the two configurations of the monomers. The steric

hindrance of the *meta* position has probably an important impact at high conversion degree, and during this step, the heating rate may have an influence on the curing mechanism. In addition, the increase in E_a value for the *para* position could also be due to a higher crosslink density, as it can be postulated from the higher degradation temperature seen in TGA and discussed later. In the literature, Pereira *et al.* performed a kinetic analysis of 2-substituted benzoxazines, and they found activation energies between 102 and 109 $kJ \cdot mol^{-1}$ for 2-substituted monomers obtained from benzaldehyde and valeraldehyde. Our results are thus in accordance with those values.[29] Interestingly, because we synthesized bifunctional monomers, we obtained a mixture of diastereomers, as described in monomer characterizations. Wang *et al.* showed a different behavior between polymerization of a unique diastereomer of benzoxazine, and a racemic mixture of both diastereomers.[30] In particular, the diasteromer mixture displayed a bimodal polymerization enthalpy, and a decrease in E_α for $0.5 < \alpha < 0.7$. Activation energy and kinetic parameters of diastereomer could be different, as illustrated by the different behavior of a single enantiomer. These results could explain the behavior observed for our 2-substituted benzoxazines; however, we could not be able to find another occurrence of the comparison of curing behavior of different diastereomers and enantiomers.

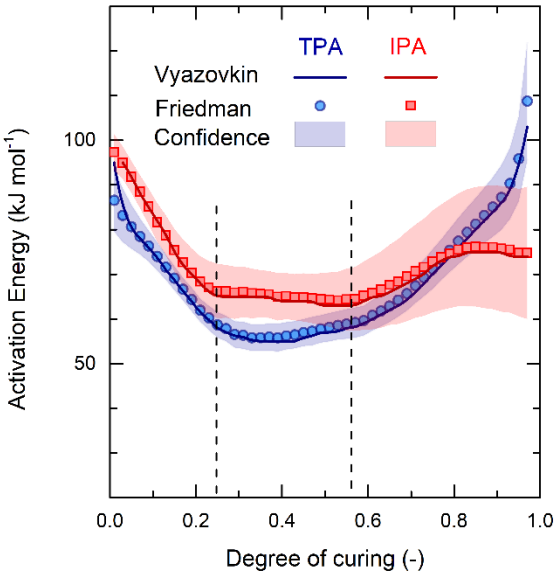

Figure 4 - Activation energy of Ph-fa[2,2']ipa and Ph-fa[2,2']tpa as a function of degree of curing, with both methods

Our results shows that model-free kinetics are suitable to analyse formaldehyde-free benzoxazines ROP. Model-free kinetics provide a better understanding of the polymerization, without requiring any hypothesis of the chemical mechanism. The apparent complexity of curing processes, revealed by the presence of bimodal signals on DSC thermograms for both monomers does not prevent the two models to give consistent results.[31] These results are in line with our work on formaldehyde-free resoles, whose crosslinking mechanisms involved several chemical reactions.[17,20,21]

3.3. ROP mechanism

FT-IR has been performed on cured samples and shows typical structure of polymerized benzoxazines, as displayed in Figure S16. Specific benzoxazine signals disappeared around 900-950 cm^{-1}, evidencing the ring-opening polymerization of both monomers. In **poly(Ph-fa[2,2']tpa)** the band at 1035 cm^{-1} disappeared while a weak band remained around 1230 cm^{-1}, and in **poly(Ph-fa[2,2']ipa)**, the 1034 cm^{-1} band disappeared and a weak band at 1226 cm^{-1} is observed revealing a typical Mannich-type linkage. This is also confirmed by the presence of a broad band around 3200 cm^{-1}, corresponding to free OH in the cured network. The disappearance of the 1585 cm^{-1} band in **poly(Ph-fa[2,2']tpa)** and the 1582 cm^{-1} signal in **poly(Ph-fa[2,2']ipa)** is attributed to the crosslinking on the furan rings.[22,23,25]

Dry content measurements allow determining if volatiles are released during polymerization, whose structural analysis is important for the determination of curing mechanism. Dry contents of **Ph-fa[2,2']tpa** and **Ph-fa[2,2']ipa** are respectively 92.4 ± 0.2 % and 89.7 ± 0.3 %, which means that smaller degassing occurs compared to formaldehyde-free benzoxazines in our previous work.[19] Our results are in accordance with Sudo *et al.* who have shown that the quantity of volatile release is higher with bulkier amine residues.[32]

Pyrolysis coupled with gas chromatography and mass spectrometry has been used in order to monitor volatiles during polymerization. Gas chromatograms for both monomers are depicted in Figure 5-a. Identification of the volatiles released during curing can be helpful for the understanding of reaction mechanisms. For both monomers, we observe one main peak with a retention time of 13.93 minutes (corresponding MS spectrum is shown in Figure 5-b). The resulting mass spectra reveals that the compound structure is an imine containing two furan groups. This result strongly suggests that after ring opening of the oxazine ring, as described in the literature, the dangling furan group from furfurylamine attacks the electrophilic iminium.[23,25,33–35] The volatilization of the compound probably occurrs from scission by ring opening of the second monomer and scission from the methylene attached to the phenol. In our latest work using Py-GC/MS analysis, we were actually not able to determine if imines were released from a single monomer or through intermolecular reaction, since our monomers were designed only from benzylic rings.[19] In this work however, the presence of an imine bearing two furan groups can only be the product of intermolecular reaction. The major product released during polymerization, as a result of furan ring attack on the iminium, reveals that this could be the most favourable reaction (Reaction scheme proposed in Figure 5-c). The furan ring is actually a better nucleophile than the phenolic ring, as it was measured by Gotta and Mayr for Friedel-Craft alkylations.[36] They calculated that methylfuran is a stronger nucleophile than O-methylated phenol (anisole). By analogy, before ring opening, one may consider that the most nucleophilic site is located on the furan. In addition, prediction of aromatic nucleophilic sites using a simulation tool (RegioSQM method)[37] for both monomer and iminium intermediates, allowed to determine that the most nucleophilic site is on the furan ring (Figure S14-S15). These comparisons would be strengthened with a DFT study of furan-containing benzoxazines, in order to better design monomers for targeted applications and better understand ring-opening polymerization of benzoxazines, as reported before.[38]

Other compounds were detected which may originate from degradation of part of the network, such as furfurylamine (retention time 5.42 min, 96 Da), methylphenols (8.56 min, 108 Da), diphenol (15.64 min, 186 Da), and an amine with furan and benzyl group (18.26 min, 201 Da). Additionally, some imines are also proposed to correspond to some detected ions, according to our previous work (8.75 min, 121 Da and 13.31 min, 109 Da). All those compounds (illustrated in Figure 5-a) are in accordance with

recent work on the volatile release during benzoxazine polymerization.[39] In overall, these structures represent a small fraction of volatiles compared to the bisfuranic imine.

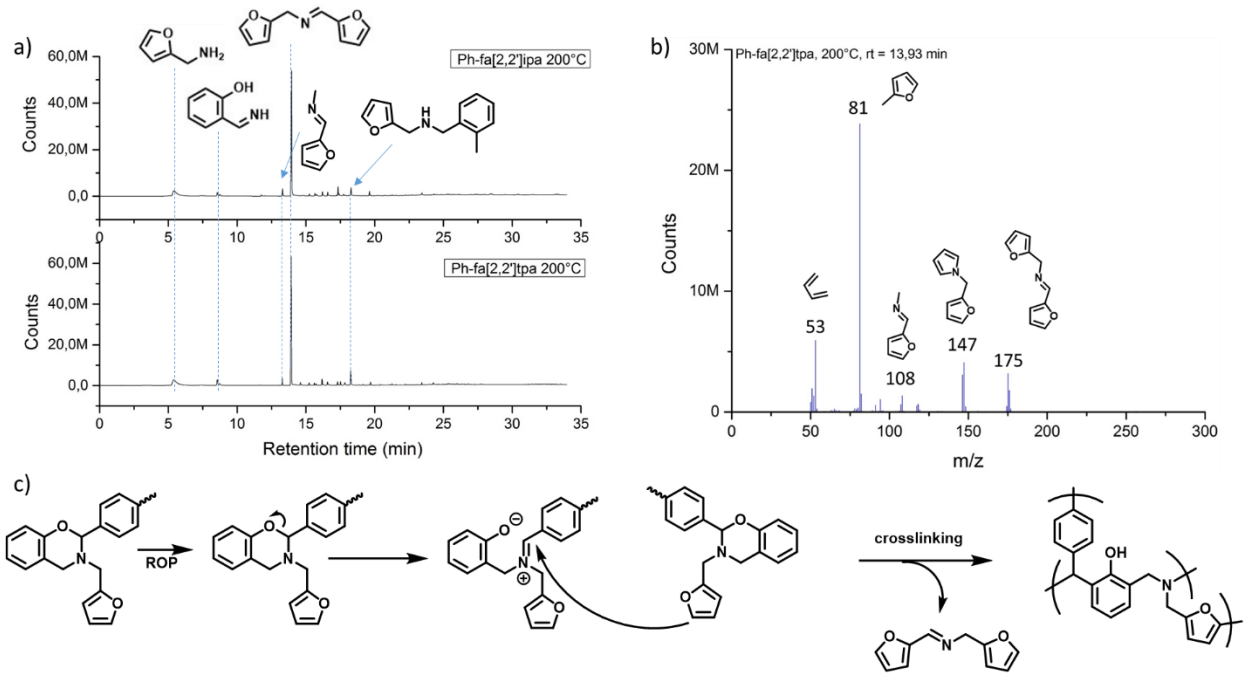

Figure 5 - a) GC chromatogram of both monomers pyrolyzed at 200°C b) MS spectrum at retention time = 13.93 minutes and c) Proposed crosslinking mechanism via *furan cycle reaction*

3.4. Thermal degradation

Thermal stability of the polybenzoxazines has been investigated by TGA under nitrogen, shown in Figure 6. The degradation study performed under nitrogen allowed the determination of char yield, that is of prime interest in the field of high performance composites.[40] Both **poly(Ph-fa[2,2'']tpa)** and **poly(Ph-fa[2,2'']ipa)** displayed the same degradation behaviour, with $T_{d10\%}$ of 412 °C and 401 °C respectively, and char yields at 900 °C of 64 % for both cured polybenzoxazines. These very interesting results evidence that both cured networks have probably the same structure, and thus the same stability. In our previous work, we reported the first synthesis of aromatic dialdehyde-based benzoxazine, which displayed 59 % of char yield.[18] Compared to **poly(Ph-fa[2,2'']tpa)** which differs only by the use of a furan ring on the amine, instead of a benzyl, it should be noted that the presence of furan ring enhances the char formation, as reported previously.[24,39] Derivative TGA (DTG), revealed the same degradation pathway, with a maximum weight loss respectively at 436 °C for **poly(Ph-fa[2,2'']ipa)** and 447 °C for **poly(Ph-fa[2,2'']tpa)**. A slight shoulder was also observed at 720 °C for both polymers, corresponding to a release of the lighter compounds during the char formation, as suggested by the pyrolysis results discussed in the last part of this article.

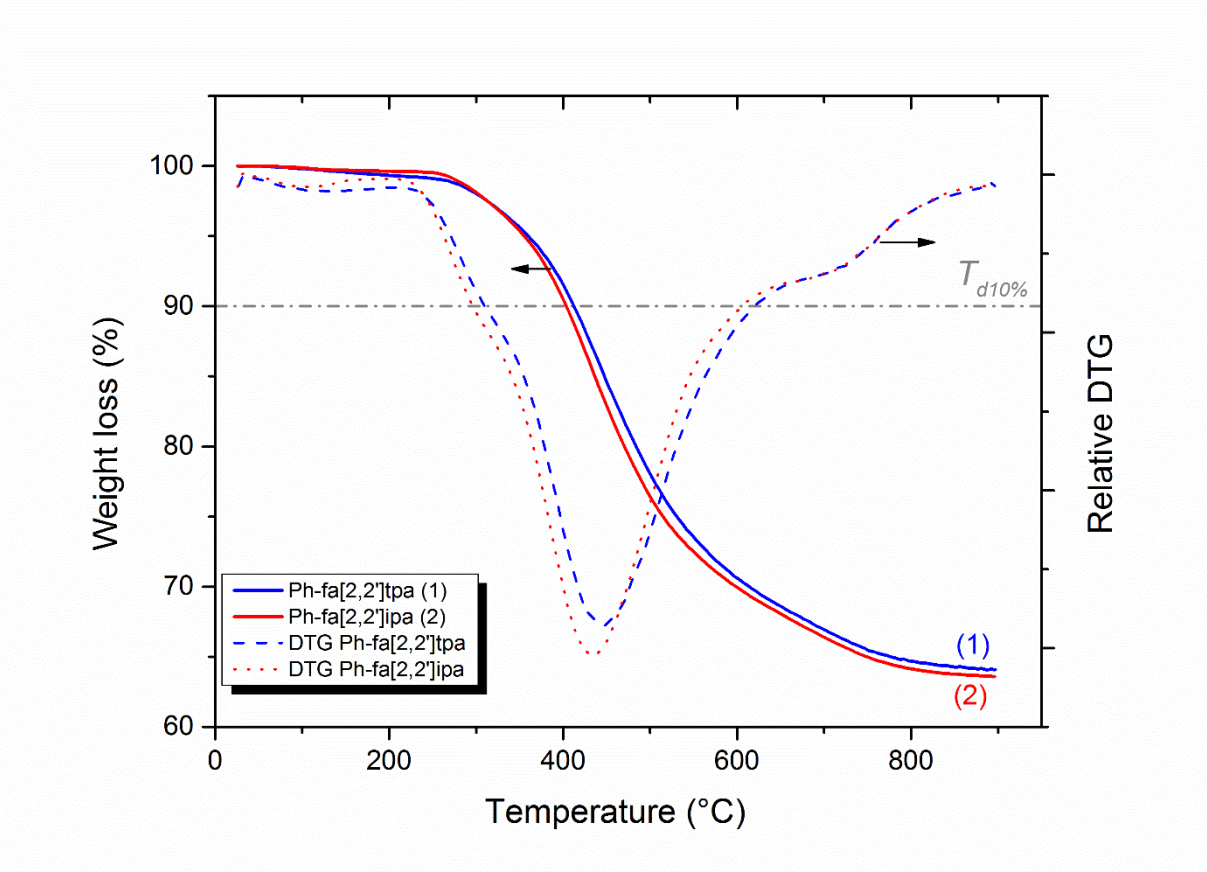

Figure 6 - TGA of cured materials under nitrogen atmosphere

The investigation of the degradation by Py-GC/MS, shown in Figure S17-S18, revealed the same degradation products from the two polybenzoxazines. Compounds such as phenol (94 Da), cresols (108 Da), xylenes (106 Da), toluene (91 Da), and benzene (78 Da) were detected. Contrary to our previous results, the release of amine or imine compounds after the pyrolysis step at 200 °C was low. This explains the higher degradation temperatures observed on DTG. The late degradation of the network is due to the higher crosslinking density, thanks to furan reaction. Aromatic compounds were released from 400°C to 900°C, with lighter aromatics at higher temperature, as we reported previously.[19] Some furanic compounds were also released, as expected. The most important degradation occurred at 500 and 600°C for both materials, in correlation with the TGA traces. These results are in line with our previous reported work, and correspond to a typical charring material, and especially polybenzoxazines.

4. Conclusion

We demonstrated the relationships between isomerism and thermal properties of two aromatic dialdehyde-based bisbenzoxazines. NMR and infrared spectroscopies revealed the structural differences between monomers, especially some intramolecular interactions. Physical properties such as melting transition was greatly influenced by the topology of the monomer. By changing the orientation of benzoxazine rings from *para* to *meta*, the melting transition was lowered by 50 °C. However, polymerization temperatures and enthalpies remained unchanged, *i.e.* with polymerization onsets of 216 °C for *para* monomer and 212 °C for *meta*, and respectively 257 $J{\cdot}g^{-1}$ (*para*) and 278 $J{\cdot}g^{-1}$

(*meta*). The reaction mechanisms investigated by Py-GC/MS were not different between the two monomers, and kinetic analyses revealed no significant difference in activation energies involved (between 55 and 103 kJ·mol^{-1}). The different kinetic regime shifts happened at the same conversion for both monomers. Finally, the degradation pathway was the same for both thermosets, with high degradation temperatures ($T_{d10\%}$ of 412 °C for *para* monomer and 401 °C for *meta*). The char formation, evidenced by Py-GC/MS, was evaluated at 64 % of the initial weight, under nitrogen. Overall, these results demonstrated that the selection of substituent is of prime importance for the control of polymerization parameters and thermal properties of polybenzoxazines. In addition, the structural conformation can help tuning the physical properties of the monomers, allowing a better control of the processability. The elaboration of formaldehyde-free polybenzoxazines with high char yields and an improved processability could be of great interest in the manufacturing of ablation composites used in aerospace industry.[40]

Supporting Information

Full ^{1}H and ^{13}C NMR spectra, ESI-HRMS of monomers, full FT-IR of cured and non-cured monomers, curing kinetics computations details, non-isothermal DSC data, SQM simulations results, GC chromatograms during degradation steps.

References

[1] B. Kiskan, Y. Yagci, The Journey of Phenolics from the First Spark to Advanced Materials, Isr. J. Chem. 60 (2020) 20–32. https://doi.org/10.1002/ijch.201900086.

[2] L. Dumas, L. Bonnaud, M. Olivier, M. Poorteman, P. Dubois, Multiscale benzoxazine composites: The role of pristine CNTs as efficient reinforcing agents for high-performance applications, Compos. Part B Eng. 112 (2017) 57–65. https://doi.org/10.1016/j.compositesb.2016.12.039.

[3] R. Andreu, J.A. Reina, J.C. Ronda, Studies on the thermal polymerization of substituted benzoxazine monomers: Electronic effects, J. Polym. Sci. Part A Polym. Chem. 46 (2008) 3353–3366. https://doi.org/10.1002/pola.22677.

[4] X. Ning, H. Ishida, Phenolic materials via ring-opening polymerization: Synthesis and characterization of bisphenol-A based benzoxazines and their polymers, J. Polym. Sci. Part A Polym. Chem. 32 (1994) 1121–1129. https://doi.org/10.1002/pola.1994.080320614.

[5] N.N. Ghosh, B. Kiskan, Y. Yagci, Polybenzoxazines—New high performance thermosetting resins: Synthesis and properties, Prog. Polym. Sci. 32 (2007) 1344–1391. https://doi.org/10.1016/j.progpolymsci.2007.07.002.

[6] Y. Yagci, B. Kiskan, N.N. Ghosh, Recent advancement on polybenzoxazine-A newly developed high performance thermoset, J. Polym. Sci. Part A Polym. Chem. 47 (2009) 5565–5576. https://doi.org/10.1002/pola.23597.

[7] S. Nalakathu Kolanadiyil, T. Endo, Toward Elucidating the Role of Number of Oxazine Rings and Intermediates in the Benzoxazine Backbone on Their Thermal Characteristics, Macromolecules. 49 (2016) 8466–8478. https://doi.org/10.1021/acs.macromol.6b01965.

[8] S. Chirachanchai, A. Laobuthee, S. Phongtamrug, Self termination of ring opening reaction of p -substituted phenol-based benzoxazines: An obstructive effect via intramolecular hydrogen bond, J. Heterocycl. Chem. 46 (2009) 714–721. https://doi.org/10.1002/jhet.130.

[9] S.N. Kolanadiyil, M. Minami, T. Endo, Synthesis and Thermal Properties of Difunctional Benzoxazines with Attached Oxazine Ring at the *Para* -, *Meta* -, and *Ortho* -Position, Macromolecules. (2017) acs.macromol.7b00487. https://doi.org/10.1021/acs.macromol.7b00487.

[10] S. Ren, X. Yang, X. Zhao, Y. Zhang, W. Huang, An m -phenylenediamine-based benzoxazine with favorable processability and its high-performance thermoset, J. Appl. Polym. Sci. 133 (2016) 43368. https://doi.org/10.1002/app.43368.

[11] A. Arnebold, O. Schorsch, J. Stelten, A. Hartwig, Resorcinol-based benzoxazine with low polymerization temperature, J. Polym. Sci. Part A Polym. Chem. 52 (2014) 1693–1699. https://doi.org/10.1002/pola.27169.

[12] H. Schäfer, A. Arnebold, J. Stelten, J. Marquet, R. María Sebastián, A. Hartwig, K. Koschek, Bifunctional benzoxazines: Synthesis and polymerization of resorcinol based single isomers, J. Polym. Sci. Part A Polym. Chem. 54 (2016) 1243–1251. https://doi.org/10.1002/pola.27966.

[13] J. Liu, H. Ishida, Anomalous Isomeric Effect on the Properties of Bisphenol F-based Benzoxazines: Toward the Molecular Design for Higher Performance, Macromolecules. 47 (2014) 5682–5690. https://doi.org/10.1021/ma501294y.

[14] C. Carré, Y. Ecochard, S. Caillol, L. Avérous, From the Synthesis of Biobased Cyclic Carbonate to Polyhydroxyurethanes: A Promising Route towards Renewable Non-Isocyanate Polyurethanes, ChemSusChem. 12 (2019) 3410–3430. https://doi.org/10.1002/cssc.201900737.

[15] A.W. Bassett, J.D. Cosgrove, K.M. Schmalbach, O.M. Stecca, C.M. Paquette, V.H. Adams, W.S. Eck, J.M. Sadler, J.J. La Scala, J.F. Stanzione, Alternative monomers for 4,4'-methylenedianiline in thermosetting epoxy resins, J. Appl. Polym. Sci. 137 (2020) 48707. https://doi.org/10.1002/app.48707.

[16] C. Mantzaridis, A.-L. Brocas, A. Llevot, G. Cendejas, R. Auvergne, S. Caillol, S. Carlotti, H. Cramail, Rosin acid oligomers as precursors of DGEBA-free epoxy resins, Green Chem. 15 (2013) 3091. https://doi.org/10.1039/c3gc41004h.

[17] L. Granado, R. Tavernier, S. Henry, R.O. Auke, G. Foyer, G. David, S. Caillol, Toward Sustainable Phenolic Thermosets with High Thermal Performances, ACS Sustain. Chem. Eng. 7 (2019) 7209–7217. https://doi.org/10.1021/acssuschemeng.8b06286.

[18] S. Ohashi, F. Cassidy, S. Huang, K. Chiou, H. Ishida, Synthesis and ring-opening polymerization of 2-substituted 1,3-benzoxazine: the first observation of the polymerization of oxazine ring-substituted benzoxazines, Polym. Chem. 7 (2016) 7177–7184. https://doi.org/10.1039/C6PY01686C.

[19] R. Tavernier, L. Granado, G. Foyer, G. David, S. Caillol, Formaldehyde-Free Polybenzoxazines for High Performance Thermosets, Macromolecules. 53 (2020) 2557–2567. https://doi.org/10.1021/acs.macromol.0c00192.

[20] L. Granado, R. Tavernier, G. Foyer, G. David, S. Caillol, Comparative curing kinetics study of high char yield formaldehyde- and terephthalaldehyde-phenolic thermosets, Thermochim. Acta. 667 (2018) 42–49. https://doi.org/10.1016/j.tca.2018.06.013.

[21] L. Granado, R. Tavernier, G. Foyer, G. David, S. Caillol, Catalysis for highly thermostable phenol-terephthalaldehyde polymer networks, Chem. Eng. J. 379 (2020) 122237. https://doi.org/10.1016/j.cej.2019.122237.

[22] C. Wang, J. Sun, X. Liu, A. Sudo, T. Endo, Synthesis and copolymerization of fully bio-based benzoxazines from guaiacol, furfurylamine and stearylamine, Green Chem. 14 (2012) 2799. https://doi.org/10.1039/c2gc35796h.

[23] P. Thirukumaran, A. Shakila Parveen, M. Sarojadevi, Synthesis and Copolymerization of Fully Biobased Benzoxazines from Renewable Resources, ACS Sustain. Chem. Eng. 2 (2014) 2790–2801. https://doi.org/10.1021/sc500548c.

[24] Y. Lu, M. Li, Y. Zhang, D. Hu, L. Ke, W. Xu, Synthesis and curing kinetics of benzoxazine containing fluorene and furan groups, Thermochim. Acta. 515 (2011) 32–37. https://doi.org/10.1016/j.tca.2010.12.014.

[25] Y.-L. Liu, C.-I. Chou, High performance benzoxazine monomers and polymers containing furan groups, J. Polym. Sci. Part A Polym. Chem. 43 (2005) 5267–5282. https://doi.org/10.1002/pola.21023.

[26] S. Vyazovkin, D. Dollimore, Linear and Nonlinear Procedures in Isoconversional Computations of the Activation Energy of Nonisothermal Reactions in Solids, J. Chem. Inf. Comput. Sci. 36 (1996) 42–45. https://doi.org/10.1021/ci950062m.

[27] H.L. Friedman, Kinetics of thermal degradation of char-forming plastics from thermogravimetry. Application to a phenolic plastic, J. Polym. Sci. Part C Polym. Symp. 6 (2007) 183–195. https://doi.org/10.1002/polc.5070060121.

[28] N. Sbirrazzuoli, Interpretation and Physical Meaning of Kinetic Parameters Obtained from Isoconversional Kinetic Analysis of Polymers, Polymers (Basel). 12 (2020) 1280. https://doi.org/10.3390/polym12061280.

[29] R.C.S. Pereira, L.R.V. Kotzebue, D. Zampieri, G. Mele, S.E. Mazzetto, D. Lomonaco, Influence of natural substituents in the polymerization behavior of novel bio-based benzoxazines, Mater. Today Commun. 21 (2019) 100629. https://doi.org/10.1016/j.mtcomm.2019.100629.

[30] J. Wang, H. Wang, J. Liu, W. Liu, X. Shen, Synthesis, curing kinetics and thermal properties of novel difunctional chiral and achiral benzoxazines with double chiral centers, J. Therm. Anal. Calorim. 114 (2013) 1255–1264. https://doi.org/10.1007/s10973-013-3081-8.

[31] N. Sbirrazzuoli, Advanced Isoconversional Kinetic Analysis for the Elucidation of Complex Reaction Mechanisms: A New Method for the Identification of Rate-Limiting Steps, Molecules. 24 (2019) 1683. https://doi.org/10.3390/molecules24091683.

[32] A. Sudo, L.-C. Du, S. Hirayama, T. Endo, Substituent effects of N-alkyl groups on thermally induced polymerization behavior of 1,3-benzoxazines, J. Polym. Sci. Part A Polym. Chem. 48 (2010) 2777–2782. https://doi.org/10.1002/pola.24026.

[33] N.K. Sini, J. Bijwe, I.K. Varma, Renewable benzoxazine monomer from Vanillin: Synthesis, characterization, and studies on curing behavior, J. Polym. Sci. Part A Polym. Chem. 52 (2014) 7–11. https://doi.org/10.1002/pola.26981.

[34] A. Trejo-Machin, A. Adjaoud, L. Puchot, R. Dieden, P. Verge, Elucidating the thermal and polymerization behaviours of benzoxazines from lignin derivatives, Eur. Polym. J. 124 (2020) 109468. https://doi.org/10.1016/j.eurpolymj.2019.109468.

[35] L. Dumas, L. Bonnaud, M. Olivier, M. Poorteman, P. Dubois, High performance bio-based benzoxazine networks from resorcinol and hydroquinone, Eur. Polym. J. 75 (2016) 486–494. https://doi.org/10.1016/j.eurpolymj.2016.01.021.

[36] M.F. Gotta, H. Mayr, Kinetics of the Friedel-Crafts alkylations of heterocyclic arenes: Comparison of the nucleophilic reactivities of aromatic and nonaromatic π- systems, J. Org. Chem. 63 (1998) 9769–9775. https://doi.org/10.1021/jo981373.

[37] J.C. Kromann, J.H. Jensen, M. Kruszyk, M. Jessing, M. Jørgensen, Fast and accurate prediction of the regioselectivity of electrophilic aromatic substitution reactions, Chem. Sci. 9 (2018) 660–665. https://doi.org/10.1039/C7SC04156J.

[38] T. Furuncuoğlu Özaltın, S. Catak, B. Kiskan, Y. Yagci, V. Aviyente, Rationalizing the regioselectivity of cationic ring-opening polymerization of benzoxazines, Eur. Polym. J. 105 (2018) 61–67. https://doi.org/10.1016/j.eurpolymj.2018.05.024.

[39] P. Wang, M. Liu, Q. Ran, The study on curing and weight-loss mechanisms of benzoxazine during thermal curing process, Polym. Degrad. Stab. 179 (2020) 109279. https://doi.org/10.1016/j.polymdegradstab.2020.109279.

[40] M. Natali, J.M. Kenny, L. Torre, Science and technology of polymeric ablative materials for thermal protection systems and propulsion devices: A review, Prog. Mater. Sci. 84 (2016) 192–275. https://doi.org/10.1016/j.pmatsci.2016.08.003.